



Closed-form FWM expressions accounting for the impact of modulation format

D. Uzunidis^{a,*}, C. Matrakidis^a, A. Stavdas^b

^a OpenLightComm Ltd, London, UK

^b Department of Informatics and Telecommunications, University of Peloponnese, Tripolis 22100, Greece

ARTICLE INFO

Keywords:

Flexgrid networks
Coherent communications
Four wave mixing
Nonlinear transmission performance

ABSTRACT

Four Wave Mixing (FWM) is one of the main transmission impairments in coherent optical systems and a broad gamut of analytical expressions calculating its power already exists in the literature. Most of these expressions, such as the GN-model, assume that due to the large values of accumulated dispersion, each transmitted signal behaves as stationary circular Gaussian noise, ignoring the dependence of FWM on the employed modulation format. This assumption leads to significant error especially in the case of quadrature-phase-shift keying (QPSK), in systems with small number of spans and in the dispersion managed case. In addition, the GN-model is inaccurate when applied to metro networks, due to the low accumulated dispersion. In this paper, we derive closed-form expressions which incorporate the impact of modulation format on FWM generation, extending and improving the accuracy compared to existing closed-form FWM expressions. Moreover, the proposed method includes terms that make it applicable to systems with small span lengths (<30 km), which is the case in metro networks. The accuracy of the proposed formulas is benchmarked against a numerical method, where the signal transmission is modeled using the split step fourier method (SSFM), for a wide range of system configurations and parameters.

1. Introduction

The demand for higher capacity transportation in Core and Metro will keep surging over the coming years due to the popularity of cloud based services, the proliferation of mobile computing and the emergence of Internet-of-Things as an asset in e-commerce. Today, optical coherent is the established technology for transportation in these network segments, but the attainable capacity times length product of the corresponding systems is limited due to fiber propagation effects. The most detrimental nonlinear propagation effect in coherent systems is FWM and it is of no surprise that a number of approximate expressions have been derived to provide an in-depth understanding [1–18].

In particular, a widely adopted approximation is the so-called GN-model [4] which postulates that, thanks to the dispersion that is accumulated along the link, each transmitted signal approximately behaves as a stationary circular Gaussian noise source. Moreover, due to this assumption, the resulting nonlinearity is independent on the employed modulation format. The GN model is accurate when large dispersion values have already been accumulated, however it results to erroneous performance estimation in systems with a small number of spans or in dispersion-managed links [14,19]. Further, as the impact of modulation format is ignored, even in the dispersion uncompensated case, a few dB discrepancy compared to numerical solutions is also

expected [19–22]. In [22–24] the Gaussian assumption of the signal is removed by including the impact of modulation format on FWM generation. As a result, the resulting expressions are more accurate than GN-model, especially in the cases of low accumulated dispersion, where the modulation format plays a role in FWM generation and its impact cannot be neglected. The main drawback of [22–24] is that the derived expressions are cumbersome and their estimation requires a non-negligible computational effort.

To overcome this limitation, a closed-form approximation of the Enhanced GN-model has been proposed in [25]. Accordingly, the closed-form EGN-model is demonstrating very good matching with numerical results, although it is suffering from certain drawbacks: it is not applicable to dispersion managed links, it leads to erroneous estimations when the span length is smaller than 30 km, while it does not account for unequal channel power, unequal bandwidth and unequal modulation format of the interacting channels. These drawbacks are making closed-form EGN-model less attractive to be incorporated in Physical Layer Aware Routing, Modulation and Spectral Assignment (PLA-RMSA) algorithms which are a key element of network optimization processes.

Herein, our primary objective is to obtain an accurate but still closed-form expression for the nonlinear FWM interference, tailored to the requirements set by PLA-RMSA algorithms in terms of computation and

* Corresponding author.

E-mail addresses: duzunidis@openlightcomm.uk (D. Uzunidis), cmatraki@openlightcomm.uk (C. Matrakidis), astavdas@uop.gr (A. Stavdas).

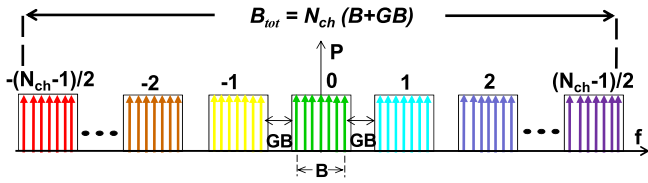


Fig. 1. Schematic diagram of a system with guard bands between the channels.

execution time. In particular, we are based on the EGN-model [22], however, we approximate it using a different mathematical procedure than the one used in [25] to derive the closed-form EGN-model. As a result, the formula derived here, compared to [25] is applicable to a wider range of system configurations and parameters: (1) it is applicable to both flexgrid and fixed-grid systems; (2) it allows to estimate the nonlinearity interference on any channel, slot or superchannel of the spectrum, not only on the central one; (3) it is applicable to both uncompensated and dispersion managed links; and (4) it is applicable to systems having channels of unequal power, unequal bandwidth and unequal modulation format.

Regarding the case of dispersion management, the GN/EGN approximations neglect the case where optical dispersion compensation means are present in a link (e.g. Dispersion Compensating Fiber — DCF set in-line or to the corresponding nodes). This is leading to erroneous estimations when such mechanisms are employed. In contrast, in the expressions derived here, we include a term, the compensation ratio (CR), that accounts for the degree of dispersion compensation induced on a link. Last, but not least, the formulation derived here is also applicable in Metro network environments where the average span length is less than 30 km, while both closed-form GN/EGN-models provide sufficient accuracy only when the fiber span loss is larger than 7 dB, which accounts for fiber lengths of 35 km or more (see Appendix F of [4] and [25]).

It is also worth mentioning that approximated expressions that calculate the impact of fiber nonlinearity have been also proposed in [6–9]. These expressions disaggregate the fiber nonlinearity into SPM, IXPM, IFWM, XPM, FWM and intersymbol or intercarrier interference and can thus be applied in different transmission systems employing direct, differential and coherent receivers. However, they are significantly more computationally complex than the formalism proposed here, making their integration with PLA-RMSA tools cumbersome.

The current work is organized as follows: in Section 2 an approximate solution for the power of the FWM interference is derived assuming a fixed grid system made up of channels with identical operational parameters (same power levels and modulation format). In Section 3, the expressions are generalized to account for a flexgrid system. In Section 4, the accuracy of the derived formulas is validated against the corresponding performance obtained from the exact numerical solutions where the transmission through the fiber is modeled using the split step Fourier method. Finally, in Section 5, more simplified and elegant expressions than those of Sections 2–3 are given that are applicable to systems with a span length longer than 40 km.

2. A fixedgrid system with channels having identical operational parameters

The system under study is schematically illustrated in Fig. 1. It consists of N_{ch} coherent optical channels with rectangular spectrum i.e. coherent optical-orthogonal frequency division multiplexing (CO-OFDM) or Nyquist-wavelength division multiplexing (Ny-WDM) with channel bandwidth equal to B and guard band between them equal to GB .

Following the methodology of EGN [22,25], a modulation dependent term is added in the expression after the original term that only assumed Gaussian statistics,

$$P_{FWM} = P_{FWM, GNA} - P_{FWM, MF} \quad (1)$$

where GNA stands for Gaussian-Noise Assumption, and MF stands for modulation format. $P_{FWM, GNA}$ and $P_{FWM, MF}$ are derived in Appendix A and the final expression is

$$P_{FWM} = \frac{32}{27} \frac{\gamma^2 L_{eff}^2 P^3 N_s^2 c}{\lambda^2 B^2 D \sqrt{z_1}} \left(1 + \frac{4e^{-aL}}{(1 - e^{-aL})^2} \right) \times \left(\operatorname{asinh} \left(\frac{\pi \lambda^2 D B^2}{8c} N_{ch} \frac{2B}{B+GB} \sqrt{z_2} \right) - \frac{5}{3} \Phi \operatorname{Log} \left(N_{ch} \frac{B}{B+GB} \right) \right) - \frac{32}{27} \frac{\gamma^2 L_{eff}^2 P^3 N_s^2 c}{\lambda^2 B^2 D \sqrt{z_1 + 12L^2}} \frac{4e^{-aL}}{(1 - e^{-aL})^2} \times \left(\operatorname{asinh} \left(\frac{\pi \lambda^2 D B^2}{8c} N_{ch} \frac{2B}{B+GB} \sqrt{z_2 + 12L^2} \right) - \frac{5}{3} \Phi \operatorname{Log} \left(N_{ch} \frac{B}{B+GB} \right) \right) \quad (2)$$

where $z_1 = \left(\frac{a}{c}\right)^2 + 2L^2 (N_s^2 - 1) (1 - CR)^2 / \left(\sum_{k=x_1}^{x_2} \frac{1}{1 + (2k\pi/(aL(1-CR)))^2}\right)^2$, $z_2 = \left(\frac{a}{c}\right)^2 + 2L^2 (N_s^2 - 1) (1 - CR)^2$, $x_1 = -\frac{\lambda^2 B^2 DL(1-CR)N_{ch}^2}{16c}$, $x_2 = \frac{\lambda^2 B^2 DL(1-CR)N_{ch}^2}{2c}$, P denotes the channel power at the fiber input, γ is the nonlinear fiber coefficient, D the local dispersion, a the fiber attenuation, L the span length and N_s the number of fiber spans in a link. CR is the dispersion compensation ratio for purely optical dispersion compensation means, like the deployment of DCF. In this case, $CR = 0$ corresponds to uncompensated transmission and $CR > 0$ to dispersion managed transmission. Φ is a modulation format depended variable taking the value of 1 for BPSK and QPSK, 17/25 for 16-QAM and 13/21 for 64-QAM [25].

3. Generalization for a flexgrid system

In this section a flexgrid system is considered where, unlike the case of Section 2, a channel might be spectrally extended over a number of frequency slots. The optical bandwidth of a frequency slot is B_{slot} and the total number of spectral slots for all active channels in a link is N_{slot} . As an example, Fig. 2 shows superchannels of 37.5 GHz and 50 GHz with $B_{slot} = 12.5$ GHz.

Under these assumptions, as elaborated in Appendix B, the power of the FWM nonlinear interference of Eq. (1) is given by

$$P_{FWM} = \frac{32}{27} \frac{\gamma^2 L_{eff}^2 P_0 N_s^2 c}{\lambda^2 B_{slot}^2 D \sqrt{z_1}} \left(1 + \frac{4e^{-aL}}{(1 - e^{-aL})^2} \right) \times \left(P_0^2 \operatorname{asinh} \left(\frac{\pi \lambda^2 D B_{slot}^2}{8c} \sqrt{z_2} \right) + \sum_{n=-\frac{N_{slot}-1}{2}, n \neq 0}^{\frac{N_{slot}-1}{2}} P_n^2 \left(1 - \frac{5}{6} \Phi_n \right) \left| \operatorname{Log} \left(\frac{n+1/2}{n-1/2} \right) \right| \right) - \frac{32}{27} \frac{\gamma^2 L_{eff}^2 P_0 N_s^2 c}{\lambda^2 B_{slot}^2 D \sqrt{z_1 + 12L^2}} \frac{4e^{-aL}}{(1 - e^{-aL})^2} \times \left(P_0^2 \operatorname{asinh} \left(\frac{\pi \lambda^2 D B_{slot}^2}{8c} \sqrt{z_2 + 12L^2} \right) + \sum_{n=-\frac{N_{slot}-1}{2}, n \neq 0}^{\frac{N_{slot}-1}{2}} P_n^2 \left(1 - \frac{5}{6} \Phi_n \right) \left| \operatorname{Log} \left(\frac{n+1/2}{n-1/2} \right) \right| \right) \quad (3)$$

where $x_1 = -\frac{\lambda^2 B_{slot}^2 DL(1-CR)N_{slot}^2}{16c}$, $x_2 = \frac{\lambda^2 B_{slot}^2 DL(1-CR)N_{slot}^2}{2c}$. The index n accounts for the number of slots of all active channels in the link and the corresponding values are in the range $-(N_{slot} - 1)/2 \leq n \leq (N_{slot} - 1)/2$. P_0 and P_n denote the total power respectively within

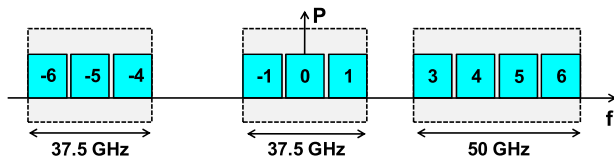


Fig. 2. Schematic diagram of a flexgrid system with 12.5 GHz grid spacing.

the measured slot and the n th interfering one. Using this expression and following the methodology analyzed in the text following Eq. (15) of [16] we can calculate the FWM power on any channel/slot of the spectrum.

Regarding the dispersion managed case, which is not handled by the GN/EGN models, the proposed expressions of (2) and (3) account for it with the CR parameter. Moreover, (2) and (3) also correct the error due to the non-Gaussian signal statistics, since they include the impact of modulation format on FWM generation, which is important in dispersion managed links due to the low values of accumulated dispersion [19]. These details make (2) and (3) applicable in the dispersion managed case whilst the approximation $i(Li_2(-ix) - Li_2(ix)) \approx \pi \operatorname{asinh}(x/2)$ used in the Appendix, instead of $i(Li_2(-ix) - Li_2(ix)) \approx \pi \operatorname{Log}(x)$ which was employed in [16], further improves the resulting accuracy over the range of $x \in (0, 10)$ which is important for dispersion managed links, systems with low span lengths and/or systems with small total bandwidth.

4. Performance estimation

Assuming that FWM is an additive Gaussian noise source, statistically independent from the signal and Amplified Spontaneous Emission (ASE) noise, we can calculate the optical signal to noise plus interference ratio (OSNIR) [4,19] as

$$OSNIR = \frac{P}{P_{ASE} + P_{FWM}} \quad (4)$$

The Bit Error Rate (BER) for QPSK and 16-QAM is estimated as

$$BER_{QPSK} = \frac{1}{2} \operatorname{erfc} \left(\sqrt{\frac{OSNIR}{2}} \right), \quad (5)$$

$$BER_{16QAM} = \frac{3}{8} \operatorname{erfc} \left(\sqrt{\frac{OSNIR}{10}} \right)$$

For other M-QAM modulation formats, the OSNIR can be related to BER using the more general formula of [26]. The total P_{ASE} for a system employing polarization multiplexing (PM) is given by $P_{ASE} = N_s h f (NF \cdot G - 1) B_0$ with B_0 the optical bandwidth and G and NF the EDFA gain and noise figure, respectively. It is worth mentioning that a phase noise component in the estimation of FWM may emerge in very low distances [27] and in this case the additive Gaussian noise assumption of (4) does not strictly apply. The impact of phase noise has a small contribution to the overall strength of FWM so it is ignored in the formulation we propose here, as an acceptable trade-off between accuracy and computational complexity which is a critical feature in PLA-RMSA algorithms.

The layout of the transportation system used to benchmark the effectiveness of the proposed solution is illustrated in Fig. 3. It consists of N_{ch} Ny-WDM polarization multiplexed channels transmitted through N_s cascaded Single Mode Fiber-Erbium Doped Fiber Amplifier (SMF)-(EDFA) pairs for the dispersion uncompensated case, whilst in the dispersion managed case the SMF is followed by an ideal Dispersion Compensating Fiber (DCF) (zero loss and nonlinearities). The simulated symbols in each case are 8192/channel/polarization. At the receiver end, the estimated BER of the two polarizations is averaged and then using (5), the OSNIR value is calculated.

We investigate fiber plants with span lengths of $L = 10, 50$ and 100 km and SMF and Non Zero Dispersion Shifted Fiber (NZDSF) with

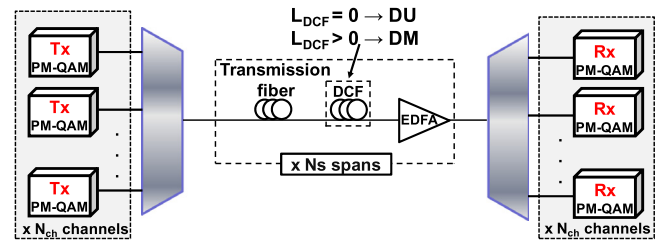


Fig. 3. Schematic diagram of the studied system. DU: Dispersion Uncompensated case, DM: Dispersion Managed case.

parameters $D = 17$ ps/(nm km), $\gamma = 1.317$ W⁻¹ km⁻¹, $a = 0.2$ dB/km and $D = 3.8$ ps/(nm km), $\gamma = 1.5$ W⁻¹ km⁻¹, $a = 0.22$ dB/km, respectively. In all cases, EDFAs with $NF = 6$ dB were used. No dispersion compensation was employed with NZDSF. Ideal optical and electrical filters and mux/demux with zero losses are considered. We also ignored the impact of polarization mode dispersion and laser linewidth. As a consequence, the dominant effects that degrade system performance are ASE noise and FWM crosstalk.

4.1. Results for a continuous range system

Fig. 4 illustrates the comparison of the proposed method of (2)–(4) against numerical results for different fiber lengths L (10, 50 and 100 km), number of spans N_s (3–50), fiber types (SMF and NZDSF), link types (uncompensated with $CR = 0$ and dispersion managed with $CR = 0.95$) and modulation formats (PM-QPSK and PM-16-QAM) in order to cover as many different scenarios as possible. The number of channels was nine each having a bandwidth of 25 GHz and a power equal to 0 dBm. This power level ensures that FWM dominates over ASE noise in all cases. For example, optimum power is always less than -3.5 dBm when the span length is 50 km for all points of Fig. 4. In the cases of 1–2 spans the BER using the numerical method was 0, so the OSNIR values were irrelevant.

As it is obvious, the uncompensated link employing SMF outperforms the dispersion managed link in all cases. This happens because in the latter case, as CR approaches 1, the FWM products generated in different spans add-up in phase, showing an increased degree of coherence and thus the FWM accumulates faster. On the other hand, when NZDSF is employed, the impact of FWM is also higher compared to SMF with $CR = 0$ which happens due to the smaller value of local dispersion D . Smaller values of D increase significantly the FWM power generation within each span [15]. Another observation is that the strength of FWM shows only a light increase with the increase of span length L . This is attributed to the fiber effective length due to which the nonlinear phenomena occur mainly in the first kilometers of the fiber (e.g. for SMF $L = 50$ and 100 km, $L_{eff} = 19.5$ and 21.5 km respectively).

Regarding the matching of the candidate formula with numerical results, it is apparent that the discrepancy is less than 1 dB in most cases whilst it hardly exceeds 1.5 dB, that is when the accumulated dispersion is very low, e.g. for span length of 10 km and less than 5 spans either for the dispersion managed case or when NZDSF is employed. The very good accuracy of the candidate approach of (2)–(4) in the cases of $L = 10$ km for more than 5 spans makes it an important asset for network engineers who aim to design or upgrade metro networks [28].

4.2. Results for different channel bandwidth

The accuracy of the proposed expressions is also validated in 12.5 GHz and 50 GHz channel bandwidth. In Fig. 5 we benchmark (2)–(4) against numerical results for a dispersion uncompensated link employing SMF fiber spans and nine channels with QPSK modulation. The channel power was properly set in each case in order to ensure that FWM dominates over ASE noise. As expected, the wider optical

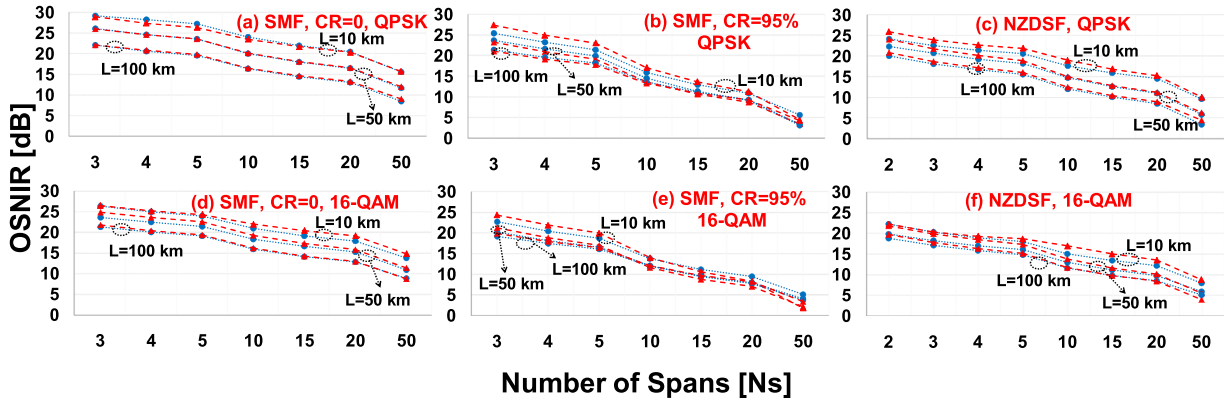


Fig. 4. OSNR value in [dB] for different configurations of a continuous spectrum system with 9 channels using the proposed method of (2)–(4) (red, triangles) and numerical solution (blue, circles). The power per channel is set to 0 dBm in all cases in order to ensure that nonlinearity dominates over ASE noise.

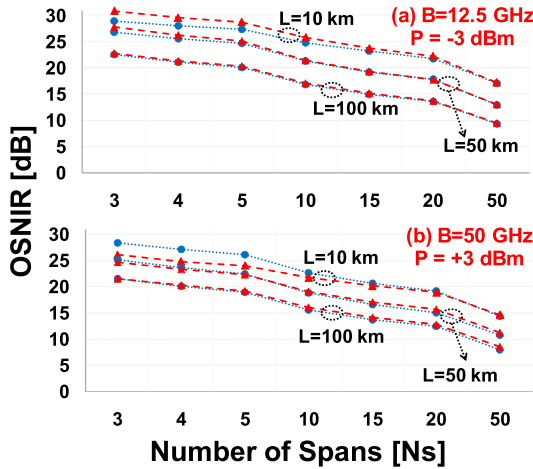


Fig. 5. Comparison of proposed method of (2)–(4) (red, triangles) with numerical solution (blue, circles) for a continuous spectrum system with 9 channels. The power per channel is properly set to ensure that nonlinearity dominates over ASE noise.

bandwidth (Fig. 5b) leads to a higher FWM crosstalk power compared to the case of a narrower bandwidth (Fig. 5a) since four times more frequencies are involved in FWM generation. As it is obvious, the accuracy of (2)–(4) is very good showing a remarkable mismatch in the case of 10 km length and for less than 10 fiber spans whilst in longer span lengths the inaccuracy is in all cases less than 1 dB.

4.3. Results at optimum channel power

Figs. 6–7 show the transparent length that can be achieved versus different power per channel for a target BER equal to 10^{-3} using (2)–(4) and the numerical solution. Throughout this work, optimum power P_{opt} is defined as the power level that maximizes the transparent length. P_{opt} depends on link parameters and in particular for $P < P_{opt}$ the link is OSNR limited while for $P > P_{opt}$ is nonlinearity limited.

Moreover, it is evident in Fig. 7 that the comparison between Fig. 7(a) with (b), (d) with (e) and (c) with (f) shows that the longer transparent length for QPSK systems with $L = 50$ km is due to the shorter distance between EDFA stages leading to slower ASE accumulation. In addition, a comparison between Fig. 6(a) with Figs. 7(b) and 6(b) with Fig. 7(e) is demonstrating the dependence of BER on modulation format where the transparent length for PM-QPSK is about four-times longer than PM-16QAM as expected from (5).

Another observation is that, comparing Fig. 7(a) with (c) and (b) with (f) SMF can achieve longer transparent lengths when compared to NZDSF. On one hand, this happens due to the higher propagation losses

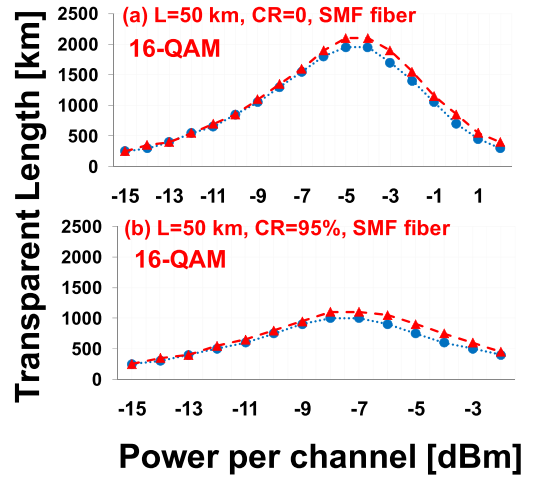


Fig. 6. Transparent length vs. channel power for a target BER of 10^{-3} using (2)–(5) (red, triangles) and numerical method (blue, circles) for different system configurations employing 16-QAM modulation format and $N_{ch} = 9$.

of the NZDSF, which lead to stronger ASE noise. On the other hand, NZDSF has lower local value of D , compared to SMF, something that leads to a lower value of accumulated dispersion per span making FWM crosstalk stronger.

Finally, it is clear that when contrasting Fig. 6(a) with (b), Fig. 7(a) with (d) and Fig. 7(b) with (e) in-line dispersion compensation mechanisms lead to significantly lower transparent lengths. This happens because the accumulated dispersion per span is low, making the FWM products generated in different spans to add-up in phase and thus strengthening the power of FWM.

An important conclusion can be drawn for the cases when accumulated dispersion is low (i.e. in NZDSF case and in dispersion managed case). In these cases the signal cannot be considered simply as a Gaussian noise source and the impact of modulation format on FWM generation should be taken into account in order to achieve accurate performance estimations. This is shown in Figs. 6–7, where the proposed expressions of (2) and (3) which include the impact of modulation format provide very good matching with numerical results.

5. Further simplifications

We can further simplify (2) and (3) given that transmission links comprise span lengths of $L > 40$ km. Then, in (8), (16)–(18) of Appendices A–B, we can approximate $1 + \frac{4e^{-aL} \sin^2\{\pi\lambda^2 B^2 jkDL/c\}}{(1-e^{-aL})^2} \approx 1$. As

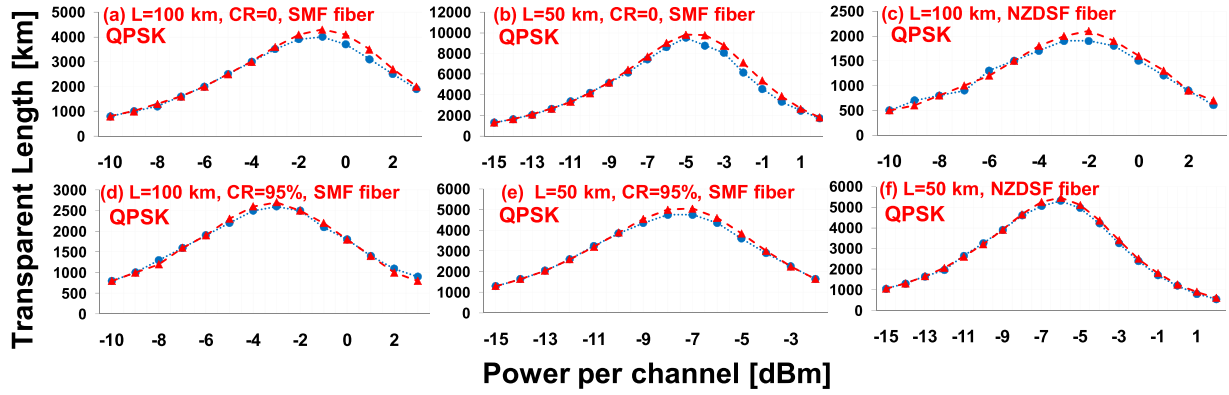


Fig. 7. Transparent length vs. channel power for a target BER of 10^{-3} using (2)–(5) (red, triangles) and numerical method (blue, circles) for different system configurations employing QPSK modulation format and $N_{ch} = 9$.

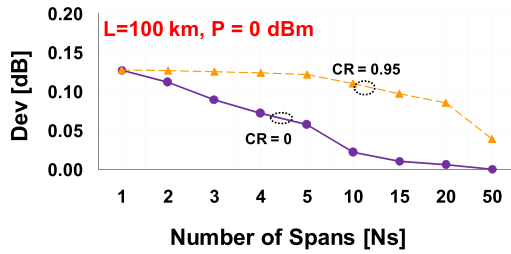


Fig. 8. Difference between (2) and (6) for 9 channels and $L = 100$ km.

such, (2) and (3) can be written, respectively, in a more convenient way

$$P_{FWM} = \frac{32}{27} \frac{\gamma^2 L_{eff}^2 P_0^3 N_s^2 c}{\lambda^2 B^2 D \sqrt{z_1}} \left(\operatorname{asinh} \left(\frac{\pi \lambda^2 D B^2}{8c} N_{ch} \frac{2B}{B+GB} \sqrt{z_2} \right) - \frac{5}{3} \Phi \operatorname{Log} \left(N_{ch} \frac{B}{B+GB} \right) \right) \quad (6)$$

$$P_{FWM} = \frac{32}{27} \frac{\gamma^2 L_{eff}^2 P_0 N_s^2 c}{\lambda^2 B_{slot}^2 D \sqrt{z_1}} \left(P_0^2 \operatorname{asinh} \left(\frac{\pi \lambda^2 D B_{slot}^2}{8c} \sqrt{z_2} \right) + \sum_{n=-\frac{N_{slot}-1}{2}, n \neq 0}^{\frac{N_{slot}-1}{2}} P_n^2 \left(1 - \frac{5}{6} \Phi_n \right) \left| \operatorname{Log} \left(\frac{n+1/2}{n-1/2} \right) \right| \right) \quad (7)$$

Evidently, the expressions (6)–(7) are much simpler compared to (2)–(3). However, despite the complexity reduction, the accuracy of (6)–(7) is sufficiently high as they estimate the power of FWM with less than 0.15 dB deviation compared to (2)–(3), when $L > 40$ km, for almost any parameter combination. This could be advantageous when rapid calculation of the physical layer performance of a network is sought. Fig. 8 shows the deviation between (2) and (6) defined as $Dev = P_{FWM, Eq. (2)} [\text{dBm}] - P_{FWM, Eq. (6)} [\text{dBm}]$. The deviation between (2) and (6) is found to be up to 0.13 dB both for the uncompensated and the dispersion managed case. To further elaborate this deviation, Dev can be approximated as $\left(1 + \frac{4e^{-aL}}{(1-e^{-aL})^2} \right) - \sqrt{\frac{z_1}{z_1+12L^2}} \frac{4e^{-aL}}{(1-e^{-aL})^2}$ considering that $\operatorname{asinh}(\cdot)$ is a slowly varying function. Recalling that z_1 is a function of $(1-CR)$, the term $\sqrt{\frac{z_1}{z_1+12L^2}}$ increases as $CR \rightarrow 0$ while it decreases as $CR \rightarrow 1$. As a consequence, Dev is lower in the dispersion uncompensated case compared to the dispersion managed case, something that is also evident in Fig. 8.

6. Conclusions

We have derived and validated the accuracy of a closed-form formula which includes the impact of modulation format on FWM generation. This method can be used to estimate the optical performance for a wide range of system configurations and parameters spanning from metro applications to long-haul and submarine transmissions. The assumption that the signal is a stationary circular Gaussian noise source can be efficient when the accumulated dispersion is significant, i.e. in dispersion uncompensated links, but it leads to erroneous estimations when the accumulated dispersion is low, i.e. in the case of metro networks, in dispersion managed links and in short links of a few hundred of kilometers. The formulation we developed here is tailored especially to these cases showing very good matching with numerical results and thus can be included in PLA-RMSA algorithms which perform multiple calculations in real-time.

Acknowledgment

This work was partially funded from the 5G-PPP METRO-HAUL project, EU grant agreement number: 761727.

Appendix A

From [29], $P_{FWM, GNA}$ for a system with guard bands between channels is given by

$$P_{FWM, GNA} = \frac{1}{1 + (2\pi \lambda^2 B^2 jkD/(ac))^2} \frac{\sin^2(N_s \pi \lambda^2 B^2 jkDL(1-CR)/c)}{\sin^2(\pi \lambda^2 B^2 jkDL(1-CR)/c)} \left(\frac{16}{27} \gamma^2 L_{eff}^2 P^3 \int_{n'=-\frac{N_{ch}-1}{2}}^{\frac{N_{ch}-1}{2}} \int_{n=\frac{n'\Delta B+B/2}{B}}^{\frac{n'\Delta B+B/2}{B}} \int_{n=\frac{n'\Delta B-B/2}{B}}^{\frac{n'\Delta B-B/2}{B}} \left(1 + \frac{4e^{-aL} \sin^2(\pi \lambda^2 B^2 jkDL/c)}{(1-e^{-aL})^2} \right) djdj \right) \quad (8)$$

where $\Delta B = B + GB$ and we also assume that $(i-k)(j-k) \approx j \cdot k$, which is accurate in a multi-channel system where the number of interfering frequencies is high. This double integral cannot be solved analytically, so some approximations have to be made. In [15,16], the following approximations were made

$$\frac{\sin^2(N_s \pi \lambda^2 B^2 jkDL(1-CR)/c)}{\sin^2(\pi \lambda^2 B^2 jkDL(1-CR)/c)} \approx N_s^2 \times \left(e^{-(N_s^2-1)(\pi \lambda^2 B^2 jkDL(1-CR)/c)^2} \right) \quad (9)$$

$$\frac{1}{1 + (2\pi \lambda^2 B^2 jkD/(ac))^2} \approx e^{-(2\pi \lambda^2 B^2 jkD/(ac))^2}$$

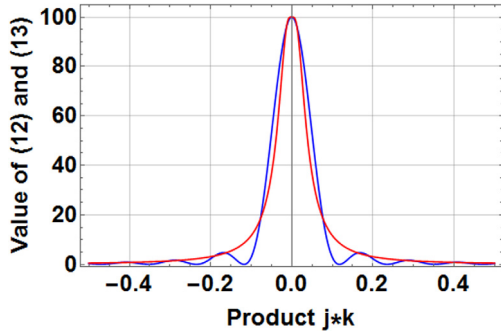


Fig. 9. Comparison of (12) (blue) with its approximation: (13) (red) for a continuous spectrum system with 9 channels and $N_s = 10$ spans of $L = 10$ km. (For interpretation of the references to color in this figure legend, the reader is referred to the web version of this article.)

The following term, can be approximated as

$$\sin^2(\pi\lambda^2 B^2 jkDL/c) = 1 - \cos^2(\pi\lambda^2 B^2 jkDL/c) \approx 1 - \left(e^{-6(\pi\lambda^2 B^2 jkDL/c)^2} \right)^2 \quad (10)$$

and as a result the product of the right side functions of (9) and (10) results to exponential functions. Then, using the Taylor approximation $e^{-x^2} \approx \frac{1}{1+x^2}$ (8) can be written as

$$P_{FWM,GNA} = \sum_{n=-\frac{N_{ch}-1}{2}}^{\frac{N_{ch}-1}{2}} \sum_{n'=-\frac{N_{ch}-1}{2}}^{\frac{N_{ch}-1}{2}} \int_{\frac{n\Delta B-B/2}{B}}^{\frac{n'\Delta B+B/2}{B}} \int_{\frac{n\Delta B-B/2}{B}}^{\frac{n\Delta B+B/2}{B}} \left(\frac{16}{27} \gamma^2 L_{eff}^2 P^3 N_s^2 \cdot \left(\frac{1}{1+(jky_1)^2} \left(1 + \frac{4e^{-aL}}{(1-e^{-aL})^2} \right) - \frac{1}{1+(jky_2)^2} \frac{4e^{-aL}}{(1-e^{-aL})^2} \right) \right) djdk \quad (11)$$

where $y_1 = \frac{\pi\lambda^2 B^2 D}{c} \sqrt{\left(\frac{2}{a}\right)^2 + 2(N_s^2 - 1)L^2(1-CR)^2}$ and $y_2 = \frac{\pi\lambda^2 B^2 D}{c} \sqrt{\left(\frac{2}{a}\right)^2 + 2(N_s^2 - 1)L^2(1-CR)^2 + 12L^2}$.

The value 6 in the power of the exponential function of (10) is a fitting parameter used to match the width of the Gaussian-like initial function (product of the left side functions of (9) and (10)) with the resulting subtraction of lorentzian functions of (11). In particular, a comparison between the initial function of (12) and its approximation of (13) can be seen in Fig. 9. As it is obvious (13) shows very good matching with the initial function (12).

$$\frac{1}{1+(2qjk/a)^2} \frac{\sin^2(N_s qjkL(1-CR))}{\sin^2(qjkL(1-CR))} \left(1 + \frac{4e^{-aL} \sin^2(qjkL)}{(1-e^{-aL})^2} \right) \quad (12)$$

$$N_s^2 \left(\frac{1}{1+(jky_1)^2} \left(1 + \frac{4e^{-aL}}{(1-e^{-aL})^2} \right) - \frac{1}{1+(jky_2)^2} \frac{4e^{-aL}}{(1-e^{-aL})^2} \right) \quad (13)$$

where $q = \pi\lambda^2 B^2 D/c$.

Next, using the following equations, the double integral of (11) can be analytically solved

$$\int \frac{1}{(x^2+m^2)} dx = \frac{1}{m} \text{ArcTan}\left(\frac{x}{m}\right) \int_{x_1}^{x_2} \frac{1}{x} \text{ArcTan}(xy) dx = \frac{1}{2} i \left((Li_2(-iyx_2) - Li_2(iyx_2)) - (Li_2(-iyx_1) - Li_2(iyx_1)) \right) \quad (14)$$

where y is a product of variables and $Li_s(-irx_1)$ denotes the polylogarithm function with $s = 2$ with $Li_s(z) = \sum_{k=1}^{\infty} \frac{z^k}{k^s}$. Next, the double sum

can be reduced to a single sum using the following approximation

$$\sum_{n=-\frac{N_{ch}-1}{2}}^{\frac{N_{ch}-1}{2}} \sum_{n'=-\frac{N_{ch}-1}{2}}^{\frac{N_{ch}-1}{2}} \left(i \left((Li_2(-iy_1 l_1 l_1') - Li_2(iy_1 l_1 l_1')) - (Li_2(-iy_1 l_1 l_2') - Li_2(iy_1 l_1 l_2')) - (Li_2(-iy_1 l_2 l_1') - Li_2(iy_1 l_2 l_1')) + (Li_2(-iy_1 l_2 l_2') - Li_2(iy_1 l_2 l_2')) \right) \right) \quad (15)$$

$$\approx 4 \sum_{n=-\frac{N_{ch}-1}{2}, n \neq 0}^{\frac{N_{ch}-1}{2}} \left(i \left((Li_2(-iy_1 l_1) - Li_2(iy_1 l_1)) - (Li_2(-iy_1 l_2) - Li_2(iy_1 l_2)) \right) + 4i \left(Li_2\left(-i\frac{y_1}{4}\right) - Li_2\left(i\frac{y_1}{4}\right) \right) \right)$$

with $l_1 = \frac{n\Delta B+B/2}{B}, l_2 = \frac{n\Delta B-B/2}{B}, l_1' = \frac{n'\Delta B+B/2}{B}, l_2' = \frac{n'\Delta B-B/2}{B}$. Then, we use the approximations $i(Li_2(-ix) - Li_2(ix)) \approx \pi \operatorname{asinh}(x/2)$, $\operatorname{asinh}(k_1) - \operatorname{asinh}(k_2) \approx \operatorname{Log}(k_1/k_2)$ and $\sum_{n=-\frac{N_{ch}-1}{2}, n \neq 0}^{\frac{N_{ch}-1}{2}} \left| \operatorname{Log}\left(\frac{n+B/(2\Delta B)}{n-B/(2\Delta B)}\right) \right| \approx 2 \operatorname{Log}\left(N_{ch} \frac{B}{\Delta B}\right)$. After that we can get a closed-form solution.

The next step is to solve $P_{FWM,MF}$ using the same methodology we used to solve $P_{FWM,GNA}$. Using Eq. (16) of [25] and since $(\int f(x) dx)^2 \approx \int f^2(x) dx$ over a small range of integration, we have that $P_{FWM,MF}$ can be written as

$$P_{FWM,MF} = \sum_{n=-\frac{N_{ch}-1}{2}, n \neq 0}^{\frac{N_{ch}-1}{2}} \int_{\frac{n\Delta B-B/2}{B}}^{\frac{n\Delta B+B/2}{B}} \int_{-1/2}^{1/2} \left(\frac{80}{81} \Phi_n \gamma^2 L_{eff}^2 P^3 \cdot \frac{1}{1+(2\pi\lambda^2 B^2 jkD/(ac))^2} \frac{\sin^2(N_s \pi \lambda^2 B^2 jkDL(1-CR)/c)}{\sin^2(\pi \lambda^2 B^2 jkDL(1-CR)/c)} \left(1 + \frac{4e^{-aL} \sin^2(\pi \lambda^2 B^2 jkDL/c)}{(1-e^{-aL})^2} \right) \right) djdk \quad (16)$$

Next, using the analysis of (9)–(14) and performing some algebra, the difference $P_{FWM,GNA} - P_{FWM,MF}$ after having included the contribution of all principal maxima with FWM terms (see paragraph after Eq. (20) in [16]), is calculated by (2).

Appendix B

Using [25] and [29], $P_{FWM,GNA}$ and $P_{FWM,MF}$ for a flexgrid system are given by

$$P_{FWM,GNA} = \sum_{n=-\frac{N_{slot}-1}{2}}^{\frac{N_{slot}-1}{2}} \sum_{n'=-\frac{N_{slot}-1}{2}}^{\frac{N_{slot}-1}{2}} \int_{n'-1/2}^{n'+1/2} \int_{n-1/2}^{n+1/2} \left(\frac{16}{27} \gamma^2 L_{eff}^2 P^3 \cdot \frac{1}{1+(2\pi\lambda^2 B_{slot}^2 jkD/(ac))^2} \frac{\sin^2(N_s \pi \lambda^2 B_{slot}^2 jkDL(1-CR)/c)}{\sin^2(\pi \lambda^2 B_{slot}^2 jkDL(1-CR)/c)} \left(1 + \frac{4e^{-aL} \sin^2(\pi \lambda^2 B_{slot}^2 jkDL/c)}{(1-e^{-aL})^2} \right) \right) djdk \quad (17)$$

$$P_{FWM,MF} = \sum_{n=-\frac{N_{slot}-1}{2}, n \neq 0}^{\frac{N_{slot}-1}{2}} \int_{n-1/2}^{n+1/2} \int_{-1/2}^{1/2} \left(\frac{80}{81} \Phi_n \gamma^2 L_{eff}^2 P^3 \cdot \frac{1}{1+(2\pi\lambda^2 B_{slot}^2 jkD/(ac))^2} \frac{\sin^2(N_s \pi \lambda^2 B_{slot}^2 jkDL(1-CR)/c)}{\sin^2(\pi \lambda^2 B_{slot}^2 jkDL(1-CR)/c)} \left(1 + \frac{4e^{-aL} \sin^2(\pi \lambda^2 B_{slot}^2 jkDL/c)}{(1-e^{-aL})^2} \right) \right) djdk \quad (18)$$

where n ranges from $-(N_{slot} - 1)/2 \leq n \leq (N_{slot} - 1)/2$ and includes only the filled frequency slots. The main differences, regarding the mathematical analysis, compared to previous case (Appendix A) are the limits of integration. The methodology and the approximations remain the same. As a consequence, the difference $P_{FWM, GNA} - P_{FWM, MF}$ for a flexgrid system after having included the contribution of all principal maxima with FWM terms (see paragraph after Eq. (20) in [16]), is calculated by (3).

References

- [1] A. Splett, C. Kurtzke, K. Petermann, Ultimate transmission Capacity of amplified optical fiber communication systems taking into account fiber nonlinearities, in: *Eur. Conf. Opt. Commun.*, 1993.
- [2] X. Chen, W. Shieh, Closed-form expressions for nonlinear transmission performance of densely spaced coherent optical OFDM systems, *Opt. Express* 18 (2010) 19039–19054, <http://www.ncbi.nlm.nih.gov/pubmed/20940798>.
- [3] G. Gao, X. Chen, W. Shieh, Analytical expressions for nonlinear transmission performance of coherent optical OFDM systems with frequency guard band, *J. Lightwave Technol.* 30 (2012) 2447–2454, <http://dx.doi.org/10.1109/JLT.2012.2200652>.
- [4] P. Poggiolini, The GN model of non-linear propagation in uncompensated coherent optical systems, *J. Lightwave Technol.* 30 (2012) 3857–3879.
- [5] M. Jaworski, M. Klinkowski, Accurate calculation of FWM noise power for ultra-dense phase modulated optical systems, in: 2012 14th Int. Conf. Transparent Opt. Networks, 2012, <http://dx.doi.org/10.1109/ICTON.2012.6253798>.
- [6] H. Song, S. Member, M. Brandt-pearce, S. Member, A 2-D Discrete-Time Model of Physical Impairments in Wavelength-Division Multiplexing Systems, 30 (2012) 713–726.
- [7] H. Song, M. Brandt-Pearce, Tingjun Xie, S.G. Wilson, Combined constrained code and LDPC code for long-haul fiber-optic communication systems, in: 2012 IEEE Glob. Commun. Conf., IEEE, 2012, pp. 2984–2989, <http://dx.doi.org/10.1109/GLOCOM.2012.6503571>.
- [8] H. Song, M. Brandt-pearce, S. Member, Range of Influence and Impact of Physical Impairments in Long-Haul DWDM Systems, 31 (2013) 846–854.
- [9] Houbing Song, M. Brandt-Pearce, Model-centric nonlinear equalizer for coherent long-haul fiber-optic communication systems, in: 2013 IEEE Glob. Commun. Conf., IEEE, 2013, pp. 2394–2399, <http://dx.doi.org/10.1109/GLOCOM.2013.6831432>.
- [10] H. Beyranvand, J.A. Salehi, A quality-of-transmission aware dynamic routing and spectrum assignment scheme for future elastic optical networks, *J. Lightwave Technol.* 31 (2013) 3043–3054, <http://dx.doi.org/10.1109/JLT.2013.2278572>.
- [11] D. Uzunidis, C. Matrakidis, A. Stavdas, Simplified model for nonlinear noise calculation in coherent optical OFDM systems, *Opt. Express* 22 (2014) 28316–28326, <http://dx.doi.org/10.1364/OE.22.028316>.
- [12] P. Johannisson, E. Agrell, Modeling of nonlinear signal distortion in fiber-optic networks, *J. Lightwave Technol.* 32 (2014) 4544–4552, <http://dx.doi.org/10.1109/JLT.2014.2361357>.
- [13] P. Poggiolini, G. Bosco, a. Carena, V. Curri, Y. Jiang, F. Forghieri, The GN-model of fiber non-linear propagation and its applications, *J. Lightwave Technol.* 32 (2014) 694–721, <http://dx.doi.org/10.1109/JLT.2013.2295208>.
- [14] Y. Qiao, M. Li, Q. Yang, Y. Xu, Y. Ji, Analytical expressions for the nonlinear interference in dispersion managed transmission coherent optical systems, *Opt. Commun.* 335 (2015) 116–125, <http://dx.doi.org/10.1016/j.optcom.2014.09.008>.
- [15] D. Uzunidis, C. Matrakidis, A. Stavdas, An improved model for estimating the impact of FWM in coherent optical systems, *Opt. Commun.* 378 (2016) 22–27, <http://dx.doi.org/10.1016/j.optcom.2016.05.022>.
- [16] D. Uzunidis, C. Matrakidis, A. Stavdas, Analytical FWM expressions for coherent optical transmission systems, *J. Lightwave Technol.* 35 (2017) 2734–2740, <http://dx.doi.org/10.1109/JLT.2017.2667722>.
- [17] D. Semrau, R. Kille, P. Bayvel, A Closed-Form Approximation of the Gaussian Noise Model in the Presence of Inter-Channel Stimulated Raman Scattering, *arXiv: 1808.07940*. (2018).
- [18] P. Poggiolini, A generalized GN-model closed-form formula, *arXiv Prepr. arXiv: 1810.06545*. (2018).
- [19] D. Uzunidis, C. Matrakidis, A. Stavdas, Comparison of simplified FWM expressions for coherent optical systems in both dispersion managed and un-managed fiber links, in: *Panhellenic Conf. Informatics*, 2016.
- [20] G. Bosco, F. Forghieri, V. Curri, A. Carena, P. Poggiolini, Impact of the transmitted signal initial dispersion transient on the accuracy of the GN-model of non-linear propagation, in: 39th Eur. Conf. Exhib. Opt. Commun. (ECOC 2013), Institution of Engineering and Technology, 2013, pp. 726–728, <http://dx.doi.org/10.1049/cp.2013.1515>.
- [21] R. Dar, M. Feder, A. Mecozzi, M. Shtaif, Accumulation of nonlinear interference noise in fiber-optic systems, *Opt. Express* 22 (2014) 14199–14211, <http://dx.doi.org/10.1364/OE.22.014199>.
- [22] A. Carena, G. Bosco, V. Curri, Y. Jiang, P. Poggiolini, F. Forghieri, EGN Model of non-linear fiber propagation, *Opt. Express* 22 (2014) 16335–16362, <http://dx.doi.org/10.1364/OE.22.016335>.
- [23] A. Mecozzi, R. Essiambre, Nonlinear Shannon limit in pseudolinear coherent systems, *J. Lightwave Technol.* 30 (2012) 2011–2024, <http://dx.doi.org/10.1109/JLT.2012.2190582>.
- [24] R. Dar, M. Feder, A. Mecozzi, M. Shtaif, Properties of nonlinear noise in long, dispersion-uncompensated fiber links, *Opt. Express* 21 (2013) 25685–25699, <http://dx.doi.org/10.1364/OE.21.025685>.
- [25] P. Poggiolini, G. Bosco, S. Member, S. Member, A. Carena, V. Curri, et al., A simple and effective closed-form GN model correction formula accounting for signal non-gaussian distribution, *J. Lightwave Technol.* 33 (2015) 459–473.
- [26] V.J. Urlick, J.X. Qiu, F. Bucholtz, Wide-band QAM-over-fiber using phase modulation and interferometric demodulation, *IEEE Photonics Technol. Lett.* 16 (2004) 2374–2376, <http://dx.doi.org/10.1109/LPT.2004.834551>.
- [27] P. Poggiolini, Y. Jiang, Recent advances in the modeling of the impact of non-linear fiber propagation effects on uncompensated coherent transmission systems, *J. Lightwave Technol.* 35 (2017) 458–480, <http://dx.doi.org/10.1109/JLT.2016.2613893>.
- [28] D. Uzunidis, C. Matrakidis, A. Stavdas, A. Lord, Dufinet: A flexible, high-Capacity and cost-effective solution for metropolitan area networks, in: *Eur. Conf. Opt. Commun.*, 2018.
- [29] K. Inoue, Phase-mismatching characteristic of four-wave mixing in fiber lines with multistage optical amplifiers, *Opt. Lett.* 17 (1992) 801–803.